Virology 394 (2009) 321–330

Contents lists available at ScienceDirect

Virology

journal homepage: www.elsevier.com/locate/yviro

Single residue deletions along the length of the influenza HA fusion peptide lead to inhibition of membrane fusion function

William A. Langley [a], Sudha Thoennes [a], Konrad C. Bradley [a], Summer E. Galloway [a], Ganesh R. Talekar [a], Sandra F. Cummings [a], Eva Varecková [b], Rupert J. Russell [c], David A. Steinhauer [a,*]

[a] Department of Microbiology and Immunology, Emory University School of Medicine, 1510 Clifton Road, Atlanta, GA 30322, USA
[b] Institute of Virology, Slovak Academy of Sciences, Bratislava, Slovak Republic
[c] School of Biology, University of St. Andrews, Fife KY16 9ST, UK

ARTICLE INFO

Article history:
Received 22 June 2009
Returned to author for revision
13 August 2009
Accepted 24 August 2009
Available online 15 September 2009

Keywords:
Influenza
Hemagglutinin
Membrane fusion
Fusion peptide

ABSTRACT

A panel of eight single amino acid deletion mutants was generated within the first 24 residues of the fusion peptide domain of the of the hemagglutinin (HA) of A/Aichi/2/68 influenza A virus (H3N2 subtype). The mutant HAs were analyzed for folding, cell surface transport, cleavage activation, capacity to undergo acid-induced conformational changes, and membrane fusion activity. We found that the mutant ΔF24, at the C-terminal end of the fusion peptide, was expressed in a non-native conformation, whereas all other deletion mutants were transported to the cell surface and could be cleaved into HA1 and HA2 to activate membrane fusion potential. Furthermore, upon acidification these cleaved HAs were able to undergo the characteristic structural rearrangements that are required for fusion. Despite this, all mutants were inhibited for fusion activity based on two separate assays. The results indicate that the mutant fusion peptide domains associate with target membranes in a non-functional fashion, and suggest that structural features along the length of the fusion peptide are likely to be relevant for optimal membrane fusion activity.

Introduction

All enveloped viruses encode glycoproteins that function to mediate fusion of their membranes with those of host cells during the initial stages of infection. Such viral fusion proteins (VFPs) are designed to respond to external stimuli at the appropriate time and place, to rearrange their molecular structures and initiate the fusion process. Membrane fusion can occur at the plasma membrane of host cells, often following the engagement of receptor molecules, or within subcellular compartments such as endosomes following internalization and acidification of the local environment (Harrison, 2008; Kielian and Rey, 2006; Lamb and Jardetzky, 2007; Weissenhorn et al., 2007; White et al., 2008). Often, more than one viral protein is involved, and for some viruses multiple cellular components take part in the fusion process. However, for most enveloped viruses a single membrane anchored VFP serves as the principal protagonist for drawing the membranes into proximity with one another to initiate the fusion event. For these VFPs, the structural rearrangements that trigger fusion are generally coincident with the exposure of relatively hydrophobic domains to allow for their interaction with cellular target membranes. These "fusion peptide" domains are known to occur in one of three basic forms; (i) they can be present at the N-terminus of the fusion subunit of the protein, (ii) they can reside within the polypeptide chain as single loop internal fusion peptide domains, and (iii) they can exist as internal bipartite loops.

Most of the VFPs that have been characterized appear to share some of the mechanistic features for bringing viral and cellular membranes into proximity with one another in the initial stages of the fusion process. However, VFPs are often segregated into three classes, based primarily on common structural considerations. Among these, representatives of Class I VFPs from members of the orthomyxoviridae, paramyxoviridae, and retroviridae families have been particularly well characterized. For these VFPs, polypeptide precursors associate to form trimers that are cleaved to generate N-terminal fusion peptides on their membrane-anchored subunit. During the fusion process, these membrane-anchored subunits undergo conformational changes to generate highly stable helical rod structures. As a consequence, the N-terminal fusion peptides are relocated to the same end of the molecule as the C-proximal viral membrane anchor domain. The molecular rearrangements and end-state structures for Class I VFPs are consistent with a model for membrane fusion, in which N-terminal fusion peptides are directed to interact with cellular target membranes, and formation of helical rod structures bring the viral and cellular membranes into proximity to one another as a prelude to the fusion process.

The influenza A virus hemagglutinin glycoprotein (HA) serves as the prototype for the Class I VFPs. It is synthesized as polypeptide chains of approximately 550 amino acids that associate non-covalently as homotrimers. The precursor form of the trimer (HA0)

* Corresponding author.
E-mail address: steinhauer@microbio.emory.edu (D.A. Steinhauer).

0042-6822/$ – see front matter © 2009 Elsevier Inc. All rights reserved.
doi:10.1016/j.virol.2009.08.031

requires proteolytic cleavage of each monomer into the disulfide-linked subunits HA1 and HA2 in order to activate membrane fusion potential and virus infectivity (Appleyard and Maber, 1974; Klenk et al., 1975; Lazarowitz and Choppin, 1975). Cleavage of HA0 not only liberates the HA2 N-terminal fusion peptide domain, but allows the HA to assume a neutral pH conformation that can subsequently be triggered by acidification to undergo the conformational changes required for membrane fusion (Bizebard et al., 1995; Bullough et al., 1994; Chen et al., 1999).

Although the fusion peptides of all Class I VFPs feature several large hydrophobic amino acids and include a number of glycine residues interspersed along their length, there is no direct sequence homology outside of the individual virus families. By contrast, the HA fusion peptide domains of all16 HA subtypes of influenza A viruses, as well as those of influenza B viruses, are highly homologous. This is particularly evident within the N-terminal 11 residues, and at positions with large hydrophobic or glycine residues (Fig. 1A). The reason for such conservation is likely due to constraints on the folding of the precursor HA0 structure, the capacity of this structure to be cleaved into a neutral pH structure that is responsive to acidification, and the requirement that fusion peptides be capable of adopting functional structures while interacting with target membranes to initiate the process of membrane fusion.

A number of studies on expressed proteins and mutant influenza viruses have focused on the membrane fusion properties of mutant HAs with changes in the fusion peptide domain (Cross et al., 2001; Daniels et al., 1985; Gething et al., 1986; Korte et al., 2001; Lai and Tamm, 2007; Lin et al., 1997; Nobusawa et al., 1995; Qiao et al., 1999; Steinhauer et al., 1995; Yewdell et al., 1993). Among the implications derived from these studies, the N-terminal glycine has been demonstrated as particularly important for fusion activity, and large hydrophobic residues at positions 2, 3, 6, 9, and 10 are desirable for optimal function. The conserved tryptophan at HA2 position 14 also appears to play a fundamental role for fusion. The glycine at position 4 has been shown to tolerate changes in functional HAs, but the glycine at position 8 may be more critical, and numerous observations suggest that the spacing of glycine residues in fusion peptides may be important for fusion peptides to adopt functional structures.

The actual length of fusion peptide domains has not been addressed in great detail, particularly as components of intact HA molecules. Experiments on mutants with a deletion of either the N-terminal glycine or the leucine at HA2 position 2 were shown to be non-functional, using assays with synthetic peptide analogs or full length expressed HAs (Steinhauer et al., 1995; Wharton et al., 1988). Further evidence for length constraints in the terminal region of the influenza fusion peptide derive from studies on cleavage activation mutants selected for growth in the presence of the protease thermolysin (Orlich and Rott, 1994). This protease cleaves HA0 between the residues that normally constitute HA2 Gly1 and Leu2, which generates an HA2 subunit with leucine at the N-terminus and a fusion peptide that is truncated by one residue. However, mutants selected for growth in the presence of thermolysin were found to contain single residue insertions just downstream of the N-terminal leucine, which functioned to restore authentic fusion peptide length.

For the present study, we extended previous analyses on the length requirements for functional influenza HA fusion peptide sequences using expressed HAs with single residue deletions that span this domain. We found that with one exception, the mutants fold into native HAs that were expressed on cell surfaces, cleaved into HA1 and HA2, and were able to undergo the acid-induced conformational changes requisite for fusion. However, all mutants were debilitated for membrane fusion function, suggesting either an overall length requirement for these fusion peptide sequences, a requirement for particular structural elements along the length of this domain, or

A. Fusion peptide sequences of representatives for each HA subtype

	1	2	3	4	5	6	7	8	9	10	11	12	13	14	15	16	17	18	19	20	21	22	23	24	25
H1	G	L	F	G	A	I	A	G	F	I	E	G	G	W	T	G	M	I	D	G	W	Y	G	Y	H
H2	–	–	–	–	–	–	–	–	–	–	–	–	–	–	Q	–	–	V	–	–	–	–	–	Y	H
H3	–	–	–	–	–	–	–	–	–	–	–	N	–	–	E	–	–	–	–	–	–	–	–	F	R
H4	–	–	–	–	–	–	–	–	–	–	–	N	–	–	Q	–	L	–	–	–	–	–	–	F	R
H5	–	–	–	–	–	–	–	–	–	–	–	–	–	–	Q	–	–	V	–	–	–	–	–	Y	H
H6	–	–	–	–	–	–	–	–	–	–	–	–	–	–	–	–	–	–	–	–	–	–	–	Y	H
H7	–	–	–	–	–	–	–	–	–	–	–	N	–	–	E	–	L	V	–	–	–	–	–	F	R
H8	–	–	–	–	–	–	–	–	–	–	–	–	–	–	S	–	–	–	–	–	–	–	–	F	H
H9	–	–	–	–	–	–	–	–	–	–	–	–	–	–	P	–	L	V	A	–	–	–	–	F	Q
H10	–	–	–	–	–	–	–	–	–	–	–	N	–	–	E	–	–	V	–	–	–	–	–	F	R
H11	–	–	–	–	–	–	–	–	–	–	–	–	–	–	P	–	L	–	N	–	–	–	–	F	Q
H12	–	–	–	–	–	–	–	–	–	–	–	–	–	–	P	–	L	V	A	–	–	–	–	F	Q
H13	–	–	–	–	–	–	–	–	–	–	–	–	–	–	P	–	L	–	N	–	–	–	–	F	Q
H14	–	–	–	–	–	–	–	–	–	–	–	N	–	–	Q	–	L	–	–	–	–	–	–	F	R
H15	–	–	–	–	–	–	–	–	–	–	–	N	–	–	E	–	L	–	–	–	–	–	–	F	R
H16	–	–	–	–	–	–	–	–	–	–	–	–	–	–	P	–	L	–	N	–	–	–	–	F	Q

B. H3 subtype fusion peptide deletion mutants for this study

	1	2	3	4	5	6	7	8	9	10	11	12	13	14	15	16	17	18	19	20	21	22	23	24	25
WT	G	L	F	G	A	I	A	G	F	I	E	N	G	W	E	G	M	I	D	G	W	Y	G	F	R
ΔL2	–	Δ	–	–	–	–	–	–	–	–	–	–	–	–	–	–	–	–	–	–	–	–	–	–	–
ΔG4	–	–	–	Δ	–	–	–	–	–	–	–	–	–	–	–	–	–	–	–	–	–	–	–	–	–
ΔI6	–	–	–	–	–	Δ	–	–	–	–	–	–	–	–	–	–	–	–	–	–	–	–	–	–	–
ΔF9	–	–	–	–	–	–	–	–	Δ	–	–	–	–	–	–	–	–	–	–	–	–	–	–	–	–
ΔN12	–	–	–	–	–	–	–	–	–	–	–	Δ	–	–	–	–	–	–	–	–	–	–	–	–	–
ΔE15	–	–	–	–	–	–	–	–	–	–	–	–	–	–	Δ	–	–	–	–	–	–	–	–	–	–
ΔD19	–	–	–	–	–	–	–	–	–	–	–	–	–	–	–	–	–	–	Δ	–	–	–	–	–	–
ΔF24	–	–	–	–	–	–	–	–	–	–	–	–	–	–	–	–	–	–	–	–	–	–	–	Δ	–

Fig. 1. A) HA Fusion peptide sequences from representatives of each of the 16 HA subtypes. H1: A/PR/8/34, H2: A/Japan/305/57, H3: A/Aichi/2/68, H4: A/Duck/Czechoslovakia/56, H5: A/Chick/Pennsylvania/1370/83, H6: A/Shearwater/Australia/1/72, H7: A/FPV/Rostock/34, H8: A/Turkey/Ontario/6118/68, H9: A/Turkey/Wisconsin/66, H10: A/Chicken/Germany/N/49, H11: A/Duck/England/56, H12: A/Duck/Alberta/60/76, H13: A/Gull/Maryland/704/77, H14: A/Mallard/Astrakhan/263/1982, H15: A/Duck/Australia/341/1983, H16: A/Black-Headed Gull/Sweden/2/99. B) Nomenclature and fusion peptide sequences of the HA deletion mutants addressed in this study. The symbol Δ denotes the deletion of the amino acid residue at this position.

constraints on the relative spacing of such elements within fusion peptide sequences.

Results and discussion

In previous studies, single residue deletion mutants of glycine at the HA2 N-terminus and leucine at position 2 have been characterized using fusion peptide analogs, expressed HAs, and laboratory-selected mutants (Orlich and Rott, 1994; Steinhauer et al., 1995; Wharton et al., 1988). The results of these studies suggest that single residue deletions at Gly1 or Leu2 lead to inhibition of fusion activity. Here we assess the structural properties and membrane fusion activity of seven additional single amino acid deletions along the length of the fusion peptide using expressed HAs derived from the parental influenza virus A/Aichi/2/68, an H3 subtype. The nomenclature and positions of deletion mutants examined in this study are shown in Fig. 1B. Fig. 1 also includes the fusion peptide sequences of representatives of the 16 HA subtypes as a reference. The ΔL2 mutant has been characterized previously, but was included in the current study as an additional control. The previous study showed that ΔL2 HA to fold properly and undergo conformational changes in response to acidic pH, but was negative for fusion activity (Steinhauer et al., 1995).

Fig. 2 shows three conformations that the HA assumes during the influenza life cycle, with fusion peptide residues highlighted in yellow. In the HA0 precursor structure, the residues that constitute the N-terminal portion of the fusion peptide form the membrane proximal half of the surface loop that is recognized by activating proteases (Chen et al., 1998). In the cleaved neutral pH HA, these residues are relocated into a cavity in the interior of the trimer, where they make contacts with ionizable residues that are thought to be significant for priming the HA for subsequent conformational changes in response to acidification (Chen et al., 1998; Thoennes et al., 2008; Wilson et al., 1981). In the low pH structure that results following the conformational changes required for fusion, the fusion peptide is relocated to the end of the helical rod structure to facilitate interaction with the target membrane (Bullough et al., 1994; Chen et al., 1999). Therefore, residues that constitute the fusion peptide provide critical roles in the context of each of the major HA conformations. The rationale behind the choice of HA2 positions for the current deletion studies was to cover the length of the HA2 N-terminal region from the N-terminus through the conserved aromatic residue (Y or F) at position 24, as residue 25 is not conserved and is often a charged or polar amino acid (Fig. 1). Individual positions for deletion were selected on the basis of previous observations on natural isolates or laboratory mutants, which showed that residues with alternative side chains at these positions were operative in fusion-positive HAs (Cross et al., 2001; Daniels et al., 1985; Gething et al., 1986; Korte et al., 2001; Lai and Tamm, 2007; Lin et al., 1997; Nobusawa et al., 1995; Qiao et al., 1999; Steinhauer et al., 1995; Yewdell et al., 1993). As such, it is unlikely that the side chains present in the WT fusion peptide at these positions are obligately required for folding of the native HA, or for fusion activity following the acid-induced conformational changes. Therefore, any consequences of their deletion are likely to result from either a decrease in the overall length of the fusion peptide, the disruption of critical motifs or structural elements within this domain, or the relative length or spacing of such features.

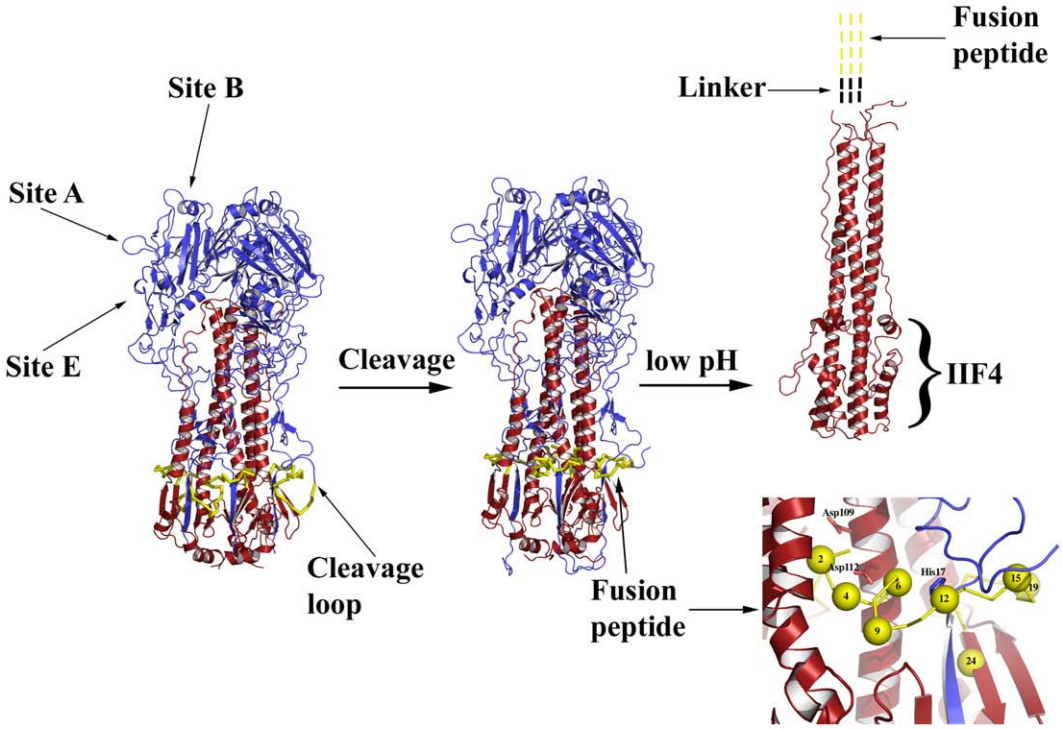

Fig. 2. Ribbon diagrams of the three conformations of the HA trimer. The HA0 precursor structure is shown on the left. Residues that will constitute the HA1 subunit following cleavage are depicted in blue, and the HA2 subunits in red. In all three structures, the residues that ultimately form the fusion peptide at the N-terminus of HA2 are shown in yellow. In the left panel, the cleavage loop of one of the HA0 monomers can be seen extending from the trimer surface and the cleavage site is indicated. The center panel shows that most of the HA structure remains unchanged following cleavage, the major structural consequence being the relocation of N-terminal HA2 "fusion peptide" residues from the bottom of the cleavage loop to the interior of the trimer. The right panel shows the structure of the HA2 trimer following the acid-induced conformational changes required for membrane fusion. In this thermostable rod-like structure, the fusion peptide and the viral transmembrane domain are located at the same end. Dashed lines indicate that the structure is unknown for both the fusion peptide and the 10-residue peptide that links it to HA2 residues of known structure. The antigenic sites A, B, and E are indicated for HA0 in the left panel, but these sites remain unchanged following proteolytic activation into the neutral pH cleaved structure shown in the center panel. The region bound by low pH HA-specific antibody IIF4 is shown in the right panel. The panel in the lower right corner depicts a magnified view of the fusion peptide region of cleaved neutral pH HA. The structural locations of HA2 residues that were deleted in this study are shown as yellow spheres. The positions of HA1 residue 17 and HA2 residues 109 and 112 are also identified.

Table 1
Antibody reactivity of cell-surface HAs by ELISA (% of WT).

	α-X31	HC100	HC159	HC31	HC68
WT	100	100	100	100	100
ΔL2	94	95	99	99	104
ΔG4	108	105	114	97	78
ΔI6	100	94	103	94	104
ΔF9	101	104	103	86	91
ΔN12	102	104	122	96	105
ΔE15	108	110	120	109	102
ΔD19	96	103	112	100	100
ΔF24	86	85	108	40	43

Values represent averages derived from at least three separate experiments.

Cell surface expression by ELISA

To analyze the effects of fusion peptide deletions on the structure and function of mutant HAs, recombinant vaccinia viruses were generated for their expression (Blasco and Moss, 1995). To assess HA folding and cell surface transport, ELISA assays were employed to determine antibody reactivity to recombinant vaccinia virus-infected HA-expressing HeLa cell monolayers. The panel of antibodies utilized included a rabbit polyclonal serum (α-X31) raised against purified trimeric HA ectodomains (BHA), and several monoclonal antibodies known to bind in conformation-specific fashion to the distinct antigenic sites A, B, or E of the HA membrane distal head domains (Daniels et al., 1983; Wiley and Skehel, 1987). The antibodies HC100 (site E), and HC159 (site A) bind to locations within the HA that remain structurally intact after the low pH conformational change occurs (Fig. 2). By contrast, the antibodies HC31 and HC68 bind to regions within site B at the membrane distal trimer interface, which are altered by de-trimerization of monomer head domains following acidification. The antibody reactivity to the mutant HA proteins is summarized in Table 1 and is represented as the percent binding compared to the WT HA as determined by OD_{450} ELISA readings. All of the mutants displayed significant reactivity with the rabbit polyclonal serum, indicating that they are capable of being transported to the cell surface. The results with the HC100 and HC159 monoclonal antibodies were consistent with this, as antibody reactivities for all mutant HAs were comparable to WT HA. However, the results with the neutral pH-specific antibodies HC31and HC68 demonstrated a significantly reduced reactivity for the ΔF24 mutant, suggesting an altered conformation for this mutant HA.

Analysis of HA0 cleavage of cell-surface HAs

The HA0 precursor protein must be cleaved into the HA1 and HA2 subunits to activate membrane fusion potential. Using the recombinant vaccinia virus system, the WT Aichi HA that we utilized in this study is expressed on the surfaces of infected cells in its uncleaved HA0 precursor form. Therefore, the capacity for cleavage activation of HA0 following exposure of HA-expressing cell monolayers to exogenous trypsin serves as an alternative assay for transport of mutant HAs to the plasma membrane. Furthermore, western blot analysis of the migration patterns of cleavage products can be used to verify that mutant proteins are processed into HA1 and HA2 subunits of characteristic size, which is a requirement for fusion function. Fig. 3 shows a western blot analysis of trypsin cleavage of WT and mutant HAs expressed on the surface of recombinant vaccinia virus-infected cells. The results demonstrate that, with the exception of the ΔF24 HA, all mutant proteins were transported to the surface of infected cells and display HA1 and HA2 cleavage products that resemble WT HA. These results, in conjunction with the ELISA data described above, suggest that the ΔF24 HA is misfolded on the cell surface relative to WT HA and the other mutants. We have observed similar results with several mutant HAs in previous studies (Li et al., 2008; Thoennes et al., 2008), and our interpretation is that such mutants are expressed on the cell surface in a conformation that is distinct from that of WT HA, and that some features of this conformation are similar to those of the low pH HA structure. HA2 residue 24 is located in the membrane distal portion of an antiparallel β-sheet structure. In a previous study designed to examine the length of peptide segment linked to the fusion peptide, many of the pairwise deletions N-terminal to HA2 residue 24 and located in the antiparallel β-sheet structure of HA0 and neutral pH cleaved HA displayed folding and expression properties similar to ΔF24 HA (Li et al., 2008).

Analysis of the pH of conformational change

Having verified that all mutant proteins except the ΔF24 HA express in native form on the cell surface and are capable of cleavage activation, we next examined the ability of the expressed HAs to undergo the acid-induced conformational changes required for fusion activity. First, we used an ELISA-based assay to assess the relative reactivities of the mutant HAs with two conformation-specific antibodies: HC3, which recognizes site A of both the neutral and low-pH HA conformations, and HC68, which preferentially binds to the neutral pH HA at site B (Fig. 2). Recombinant vaccinia virus-infected HeLa cells that were expressing HA0 on the cell surface were treated with trypsin to cleave HA0 into HA1 and HA2, washed with PBS, and incubated with PBS/citrate buffers in increments ranging in pH from 5.6 down to 4.5. Monolayers were then neutralized, fixed, and assessed for reactivity to HC68 and HC3 by ELISA. The relative ratios of HC68 to HC3 reactivity as determined by ELISA OD_{450} were plotted as a function of pH and are shown in Fig. 4. A reduction in these ratios is indicative that the HA can undergo the acid-induced conformational changes required for membrane fusion. The results demonstrate that the Δ24F HA binds poorly to HC68 at all pH values examined, confirming that this mutant is expressed in an altered conformation on the cell surface. Most other mutants exhibited a decrease in HC68:HC3 reactivity over the range of pH reductions that were tested, indicating that they are capable of undergoing the characteristic conformational changes associated with membrane fusion. The reactivity profile for the ΔE15 and ΔD19 HA mutants are not significantly different from that of WT HA, indicating that they

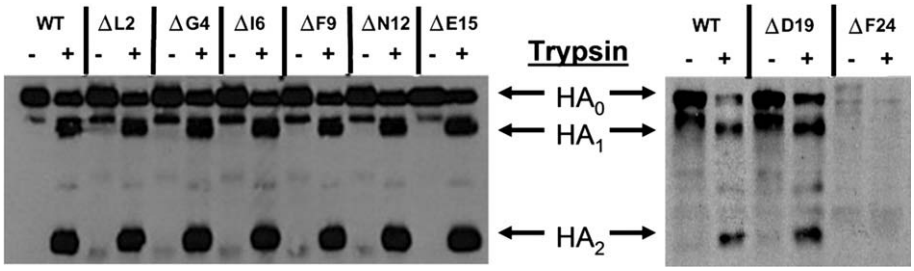

Fig. 3. Cell surface expression of HAs as assayed by trypsin cleavage of HA0 into HA1 and HA2. Recombinant vaccinia virus-infected HA-expressing cell monolayers were incubated with or without trypsin and cell lysates were analyzed by western blot following SDS-PAGE under reducing conditions.

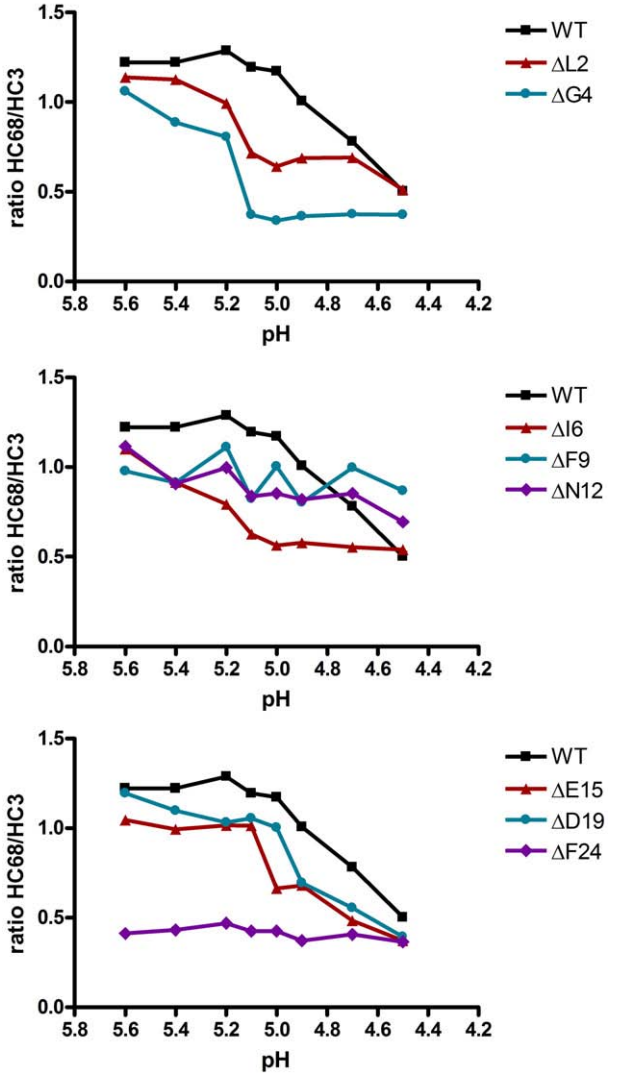

Fig. 4. Graphs of ELISA experiments to demonstrate HA conformational changes resulting from incubation at reduced pH. Graphs plot the ratios of HC68/HC3 reactivity as a function of pH. HC68 binds well with neutral pH HA, but poorly to the low pH structure. HC3 binds equally well with both HA conformations.

undergo conformational changes at a similar pH. The ΔL2 HA clearly displayed an elevated pH of conformational change relative to WT HA, confirming results that were obtained in a previous study (Steinhauer et al., 1995). Similarly, the ΔG4 and ΔI6 also appear to undergo structural rearrangements at elevated pH compared to WT. This suggests that these mutations might alter interactions that occur in native WT HA between fusion peptide residues and those located in the trimer interior, resulting in a less stable neutral pH structure. Previous reports demonstrate that a majority of fusion peptide substitution mutants with changes within the first 10 N-terminal residues of HA2 display an elevated pH of conformational change (Cross et al., 2001; Daniels et al., 1985; Gething et al., 1986; Lin et al., 1997; Qiao et al., 1999; Steinhauer et al., 1995). This is likely due to the fact that fusion peptide residues in this region make extensive contact with ionizable residues such as HA1 H17, HA2 D109, and HA2 D112 in this region of neutral pH HA following HA0 cleavage. The aspartic acid side chains of HA2 residues 109 and 112 form multiple hydrogen bonds with residues 1 through 5 of HA2, and HA1 H17 forms hydrogen bonds via a water molecule with HA2 residues 6 and 10. Therefore, the deletion of residues L2, G4, I6, or F9 could result in the disruption of one or more of the interactions between fusion peptide residues and ionizable residues in the neutral pH structure, thus destabilizing the neutral pH structure.

The pH profile observed for the ΔF9 HA was somewhat aberrant compared to the others, and was not consistent with a loss of HC68 reactivity at reduced pH, even though this mutant appeared to be expressed in the correct conformation on the surfaces of infected cells and was efficiently cleaved into HA1 and HA2. In addition, the ΔI6 and ΔN12 mutant HAs displayed a gradual loss of HC68 reactivity over a broader range of pH than we generally observe for WT and most other mutant HAs. The disruption of interactions with HA1 H17 could offer a possible explanation for this, as HA1 H17 has been implicated previously for its potential role in the initial triggering of the acid-induced conformational changes (Thoennes et al., 2008). A further examination of the capacity for these mutants to undergo structural rearrangements was carried out using an alternative conformation-specific monoclonal antibody, IIF4. This anti-peptide antibody was generated against residues 125-175 of the HA2 subunit and binds preferentially to the low-pH form of the protein at the end of the helical rod structure opposite to the fusion peptide (Vareckova et al., 2002; Wharton et al., 1995). As shown in Fig. 5, an increase in IIF4 reactivity upon reduction in pH can be observed for ΔI6, ΔF9, and ΔN12, as well as other HAs, indicating that structural rearrangements have occurred.

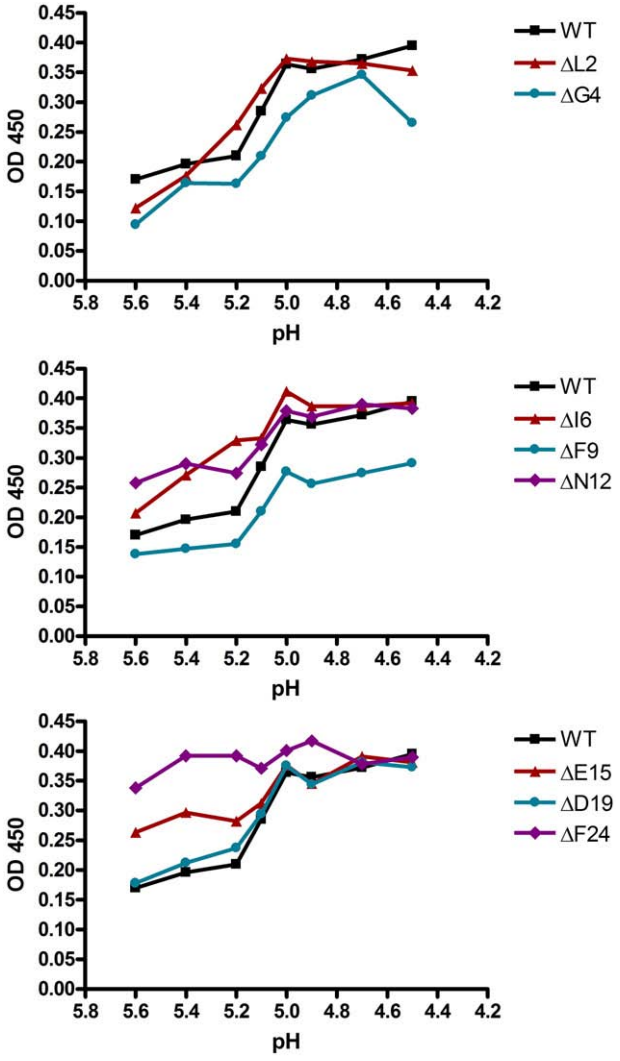

Fig. 5. Graphs of ELISA experiments showing reactivity with the low pH-specific monoclonal antibody IIF4 as a function of pH.

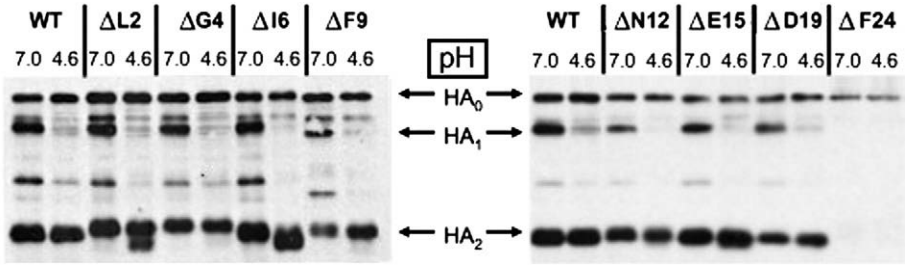

Fig. 6. Western blot analysis for the determination of the pH of conformational change by trypsin susceptibility. HA expressing cells were treated with trypsin to cleave HA0, washed, pH was adjusted to pH 4.6, and monolayers were again treated with trypsin. Lysates were then analyzed by western blot following SDS-PAGE under reducing conditions. The disappearance of HA1 bands indicates that the HA conformational changes have been triggered.

To confirm the antibody reactivity data regarding the capacity of mutant HAs to undergo acid-induced conformational changes, we carried out trypsin digestion experiments on cleaved HAs at neutral pH, or following incubation at pH 5.0. Once the HA0 precursor has been cleaved into HA1 and HA2, the WT protein is resistant to further protease digestion at neutral pH. However, upon acidification, the structural changes render the molecule susceptible to digestion by a variety of proteases, including trypsin (Skehel et al., 1982). For this experiment, HA-expressing cell monolayers were initially treated with trypsin to cleave HA0 into HA1 and HA2, as described for Fig. 3. The monolayers were then washed, and either subjected to an additional round of trypsin digestion at pH 7.2, or incubated at pH 4.6 prior to further trypsin treatment. Cell lysates were prepared and analyzed by SDS-PAGE under reducing conditions. Fig. 6 shows that the HA1 subunit of all mutants was digested by trypsin if the cleaved HA had been exposed to acidic pH, demonstrating that the mutants had gone through the characteristic conformational changes required for fusion activity. For the neutral pH samples, the results of HA1 digestion for ΔF24 HA confirm our interpretation that this HA is expressed in an altered conformation. However, the results with the ΔF9 HA indicate that neutral pH HA1 was partially degraded by the second trypsin digestion, as an additional band above HA2 was observed, which is not present in the other samples. This product is not observed during initial trypsin cleavage of HA0 into HA1 and HA2 at neutral pH (Fig. 3). This suggests that the ΔF9 HA may be unstable relative to WT and most other mutant HAs, and this could explain the aberrant results for HC68:HC3 antibody reactivities observed for the experiments shown in Fig. 4. The conformational changes required for fusion occur within seconds for WT Aichi HA, and the digestion of ΔF9 HA1 was still incomplete after two rounds of trypsin treatment over several minutes. Therefore, it is quite possible that cell surface expressed ΔF9 HA, or at least a significant percentage of it, would be capable of going through the structural rearrangements required for fusion despite inherent instability. Cumulatively, the data suggest that all deletion mutants other than ΔF24, and possibly ΔF9 HA, are expressed and folded properly, and are capable of undergoing the acid-induced structural rearrangements requisite for membrane fusion.

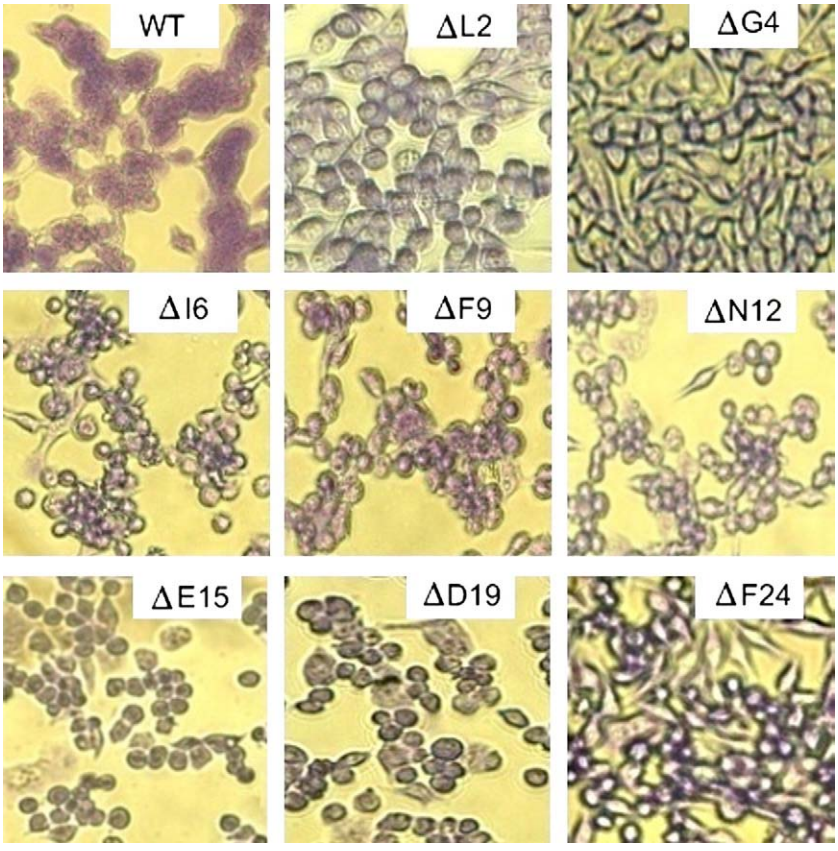

Fig. 7. Polykaryon formation by HA-expressing BHK cells following incubation at pH 4.8.

Analysis of membrane fusion by polykaryon formation and dye transfer assays

The ability of the mutant proteins to mediate fusion was assessed using an assay for polykaryon formation by recombinant vaccinia virus-infected HA-expressing BHK21 cell monolayers. HA-expressing cells were treated with trypsin to cleave HA0, the pH was adjusted by incubation in PBS/citrate buffer, monolayers were then incubated in complete medium at neutral pH, and monolayers were monitored for polykaryon formation by light microscopy. Over multiple independent experiments, no significant polykaryon formation was detected for any of the mutant HAs, even when tested in pH increments down to 4.2. Fig. 7 shows representative fields of cells for one such assay carried out at pH 4.8, which provides evidence that all mutants were inhibited for membrane fusion activity.

To confirm these results, a dye transfer assay was also performed using the fusion peptide deletion mutants. For this assay, human erythrocytes were labeled with two dyes, the lipophilic probe R18 and the soluble dye calcein (Ellens et al., 1990; Morris et al., 1989). These loaded erythrocytes were allowed to adhere to HA-expressing cell monolayers, washed, and the pH of the monolayers were adjusted. The dyes are transferred from the smaller erythrocytes to the larger HA-expressing HeLa cells if the HA is capable of mediating fusion. The transfer of R18 is indicative of lipid mixing, and the transfer of calcein demonstrates content mixing and therefore, biologically relevant fusion activity. The transfer of R18, but not calcein is indicative of a "hemifusion" phenotype, in which the lipid mixing stage of membrane fusion does not proceed to full fusion with content mixing (Kemble et al., 1994). The dye transfer assays were carried out multiple times with the deletion mutants, and results for one such experiment are shown in Fig. 8. None of the mutants were found capable of mediating WT levels of membrane fusion using this assay. No evidence for calcein transfer and content mixing was observed for any mutant at all pH examined. However, for the Δ15 and Δ19 mutants, R18 transfer was detectable at levels above background in some examples, suggesting that these mutants might be capable of hemifusion activity, as has been observed for particular HA mutants in previous studies (Cross et al., 2001; Kemble et al., 1994; Qiao et al., 1999). Dye transfer experiments were repeated in the presence of chlorpromazine (CPZ) in attempts to induce the transition from a hemifusion to full fusion state (Melikyan et al., 1997); however, these did not allow us to further define the mutant phenotypes. Concentrations of CPZ ranging from 0.1 mM to 0.5 mM were tested, and at the lower concentrations no changes in fusion properties were detected,

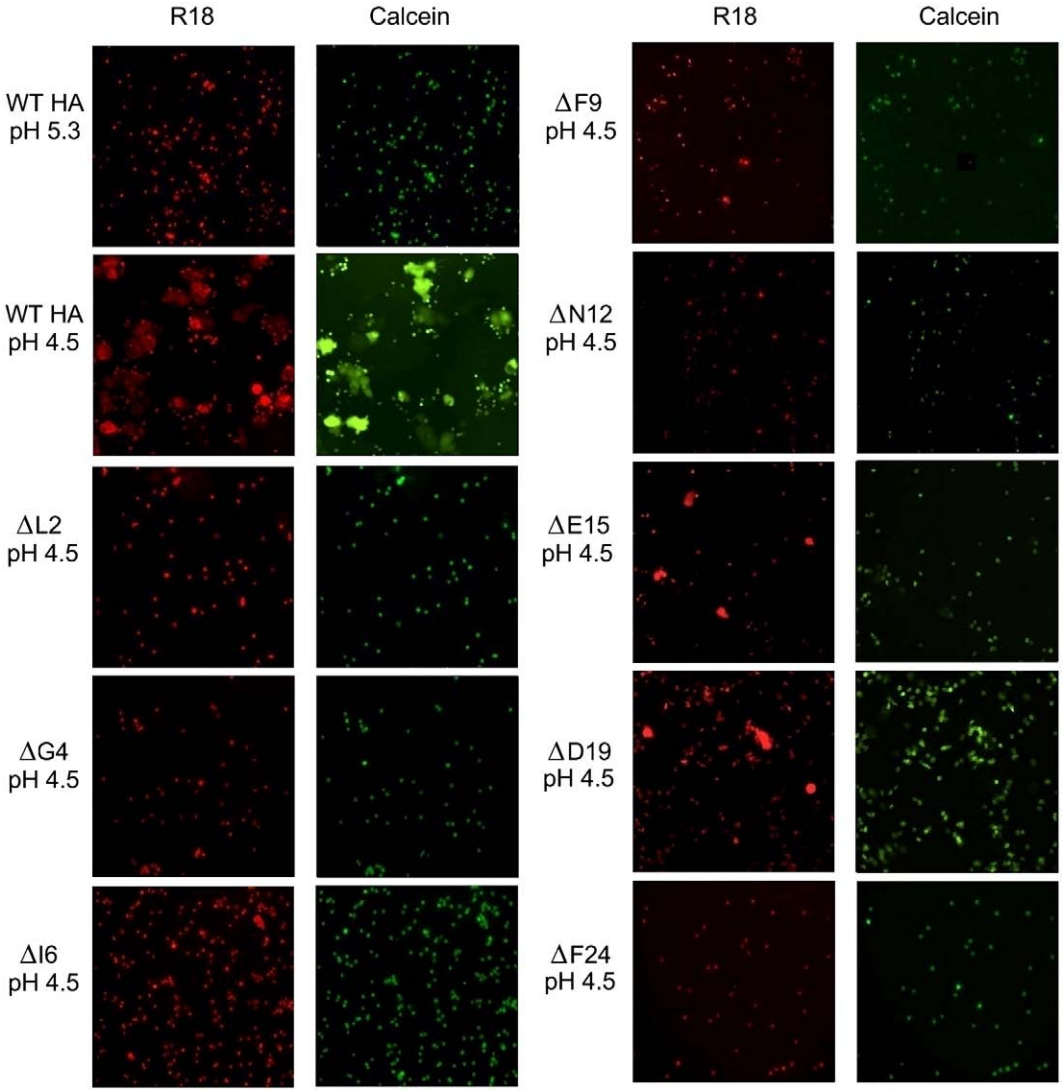

Fig. 8. Dye transfer assay for hemifusion and full fusion activity of HA mutants. Human erythrocytes loaded with R18 and calcein were adsorbed to HA-expressing cells and exposed to acidic pH to monitor HA mediated transfer of the lipid-soluble red dye R18 (lipid mixing) or the water-soluble green dye calcein (content mixing).

whereas at higher concentrations the compound appeared to cause cytopathology of the HA-expressing cells (data not shown).

One of the most well characterized of the "hemifusion" HA mutants is the fusion peptide substitution mutant G1S at the HA2 N-terminus. This serine mutant was found to display hemifusion activity by White and colleagues (Qiao et al., 1999) and in our laboratory (Cross et al., 2001), and the biophysical and structural properties have also been analyzed for G1S fusion peptide analogs (Li et al., 2003, 2005). Despite the well-documented hemifusion phenotype, we were able to rescue the HA2 G1S mutant as an infectious virus (Cross et al., 2001). However, this mutant was severely attenuated for replication, and it rapidly reverted to WT despite the requirement for two nucleotide substitutions to do so. This suggests that, while such mutants provide useful tools for dissecting the mechanistic stages of fusion at the biophysical level, they are likely to be irrelevant in any natural environment.

Deletion mutants and models for fusion peptide structure

Overall, our studies suggest that the length of the fusion peptide domain of influenza HA can influence the functional properties of the molecule at different levels, but appears to be most critical for the latter stages of fusion when this domain interacts with target membranes. All mutants except the ΔF24 HA were expressed in native conformation on the cell surface, can be cleaved into HA1 and HA2, and could be triggered by acidification to undergo the structural changes required for membrane fusion. Therefore, the most profound effects of the deletions are likely to involve the structure that these domains adopt in association with target membranes. The structure of the fusion peptide domain associated with membranes in the context of full length HA is unknown. The structure of the HA transmembrane anchor domain near the C-terminus of the molecule is also unknown, and there is evidence that this domain may also have a role in fusion (Armstrong et al., 2000; Chang et al., 2008; Melikyan et al., 2000).

Hydrophobic photolabeling analyses have indicated that the 22 N-terminal residues of HA2 interact with target membranes during fusion, and the periodicity of labeling suggests that this segment adopts an amphipathic α-helical structure (Durrer et al., 1996; Harter et al., 1989). Circular dichroism and FTIR spectroscopy studies with membrane-bound fusion peptide analogs indicated that they may contain from 40% to 60% α-helical structure, with some studies also suggesting the presence of β-structure (Gray et al., 1996; Han et al., 1999; Lear and DeGrado, 1987; Murata et al., 1987; Rafalski et al., 1991; Wharton et al., 1988). In some of these studies, a loose correlation between helical content and fusogenicity was observed (Burger et al., 1991; Lear and DeGrado, 1987; Wharton et al., 1988).

The oligomeric state adopted by fusion peptide domains in association with target membranes remains to be determined, and models involving monomeric peptides, trimeric peptides, and fusion peptides complexed with HA transmembrane domains have been proposed. Experiments using spin-labeling electron paramagnetic resonance (EPR) techniques with cysteine mutants of the fusion peptide region suggest that they associate with membranes in monomeric form (Macosko et al., 1997). Monomeric fusion peptide structures have also been proposed by Tamm and colleagues based on work with synthetic fusion peptide analogs containing a seven residue solubilization domain (GCGKKKK) attached to the C-terminal end of the first 20 residues of HA2 (Han et al., 2001; Han and Tamm, 2000; Lai et al., 2006; Lai and Tamm, 2007; Li et al., 2005). These synthetic peptides have been shown to possess pH-dependent membrane fusion activity, and their NMR structures in DPC micelles showed that the WT peptide adopted an inverted V-shaped structure at both neutral pH and pH 5.0, with the apex of the V located at the aqueous interface (Han et al., 2001). In the neutral pH structure, an N-terminal helix comprised of residues L2 to F9 is followed by a turn, which is stabilized by hydrogen bonds formed by residues G8 and F9 with residues E11 and N12. In the C-terminal portion of the peptide, residues W14-G20 form an extended structure with a bend between residues G16 and M17. By comparison, in the pH 5 structure, residue I10 extends the N-terminal helix and the turn region C-terminal to this helix contains a slightly more acute bend. This kink region may be stabilized by hydrophobic interactions between F9 and W14. Additionally, the C-terminal half of the fusion segment folds into a short 3_{10} helix, and residues E15 and D19 are reoriented such that apolar residues become aligned at the bottom face of the kinked peptide. This generates a hydrophobic pocket, and allows the peptide to assume a more closed and deeply inserted structure within the membrane at acidic pH. NMR structural studies on mutant fusion peptide analogues that are inhibited for fusion activity suggested a structural significance for the hinge region that lies in the middle of the fusion peptide sequence (Hsu et al., 2002; Lai et al., 2006; Lai and Tamm, 2007; Li et al., 2005). In the context of these structures, the deletion mutants analyzed in our current study would clearly disrupt structural features that may be critical for function, including the N-terminal alpha-helical domain, the bend region, or the orientation or presence of acidic residues at positions 15 and 19.

Other studies and models suggest that fusion peptides associate with membranes in oligomeric form. Experiments with HA fusion peptide analogs linked to coiled coil domains designed to promote their trimerization, indicate that the trimeric peptides promote a greater degree of liposomal content leakage and membrane mixing than the monomeric form (Lau et al., 2004). A series of studies by Chang and colleagues indicated that influenza HA fusion peptides can loosely assemble in lipid bilayers (Chang et al., 2000, 2008; Cheng et al., 2003), but further suggested that they form oligomeric complexes with the HA transmembrane domains when both species are present. These results are consistent with a role for the HA transmembrane anchor domain in the fusion process, as suggested by mutagenesis studies (Armstrong et al., 2000; Chang et al., 2008; Melikyan et al., 2000).

Our results with recombinant influenza virus mutants within the first 10 residues of the fusion peptide (Cross et al., 2001) are compatible with a model in which helical fusion peptides orient such that the relatively polar glycine residues form a trimeric interface, and the large hydrophobic side chains of residues 2, 6, and 10 reside on the surface to interact with membrane lipids (Skehel et al., 2001). In fact, many of the studies and models cited above suggest that the N-terminal region of the fusion peptide domain is predominantly α-helical. However, in the absence of structural information on fusion peptide and transmembrane domains associated with membranes in the context of full-length HA molecules, these models will continue to be speculative. Regardless, our results with the deletion mutants reported here suggest that structural elements along the length of the fusion peptide, or the spacing or orientation of such elements relative to one another, are critical for a functional association of fusion peptide sequences with target membranes during the fusion process.

Materials and methods

Mutagenesis and expression of HAs

The HA cDNA from the H3N2 subtype virus A/Aichi/2/68 was mutated by site-directed mutagenesis using a QuikChange mutagenesis kit (Stratagene). The presence of the desired mutations and the absence of extraneous mutations were confirmed by nucleotide sequencing of entire HA coding regions. The mutant cDNAs were expressed as recombinant vaccinia viruses using the plaque-selection system (Blasco and Moss, 1995). The generated viruses were propagated on CV1 cells in Dulbecco's modified Eagle's medium (DMEM) supplemented with 10% fetal bovine serum (FBS).

Cell surface expression trypsin cleavability and ELISA

HA cell surface expression was analyzed using a trypsin cleavage assay with recombinant vaccinia-infected CV1 cells as described previously (Steinhauer et al., 1995), except that blots were developed using chemiluminescence rather than radiolabeled secondary antibody. Following electrophoresis, blots were incubated with anti-HA rabbit polyclonal rabbit serum, washed, and incubated with a Protein A-HRP conjugate (Sigma cat# P8651). Blots were developed with the Enhanced Chemiluminescence Reagent (Amersham Pharmacia) according to the manufacturer's instructions. Quantitative cell surface expression by ELISA was carried out on recombinant vaccinia virus-infected HA-expressing HeLa cells using a panel of monoclonal antibodies that recognize distinct antigenic regions of wild-type HA as described (Steinhauer et al., 1991).

Conformational change analysis by ELISA and trypsin digestion

Analysis of conformation changes was performed on recombinant vaccinia-infected HeLa cell monolayers by ELISA using monoclonal antibodies HC3 and HC68 as described previously (Steinhauer et al., 1991). HC3 recognizes both native and low pH HA, while HC68 recognizes only the native conformation. Trypsin susceptibility of low-pH HAs were determined as described previously (Thoennes et al., 2008).

Polykaryon formation and dye transfer assays for membrane fusion activity

The pH of membrane fusion was assayed by polykaryon formation as described previously (Steinhauer et al., 1991, cited by in Scopus (39)). For dye transfer assays, fresh heparinized human erythrocytes (HRBCs) were co-labeled with the membrane probe octadecyl rhodamine B chloride (R18) and the aqueous dye calcein-AM (Sigma) as described previously (Ujike et al., 2005). Ten milliliters of freshly prepared HRBCs (1% in Dulbecco's phosphate-buffered saline [DPBS]) was mixed with 10 μl of R18 (2 mM in ethanol) with vigorous shaking. The mixture was incubated in the dark for 30 min at room temperature, followed by the addition of 30 ml of 7.5% FBS- DMEM for 20 min at room temperature to remove unbound R18. The R18-labeled HRBCs were washed three times and resuspended in DPBS (4% R18-labeled HRBCs). A 10-μl aliquot of 4 mM calcein-AM in dimethyl sulfoxide was added to 1 ml of 4% R18-labeled HRBCs in the dark and incubated at 37°C for 1 h, followed by the addition of 30 ml of 7.5% FBS-DMEM for 20 min at room temperature, three washes with DPBS to remove unbound calcein, and resuspension in DMEM (0.02% HRBCs). To analyze hemifusion and fusion pore formation by wildtype HA and HA mutants, an R18 and calcein transfer assay was performed. Recombinant vaccinia virus-infected HeLa cells expressing HA were pretreated with neuraminidase (NA) (30 mU/ml; Sigma) at 37 °C for 60 min, washed once with DPBS, and treated with TPCK-trypsin (5 μg/ml) at 37 °C for 5 min. Cells were washed with soybean trypsin inhibitor (5 μg/ml), washed, and incubated with R18- and calcein-labeled HRBCs at room temperature for 30 min for hemadsorption. After unbound HRBCs were removed by three washes, the cells were washed and incubated for 1 min at 37 °C in low-pH buffer (10 mM HEPES, 20 mM sodium citrate [pH 5.0], 150 mM NaCl, 2 mM $CaCl_2$, and 20 mM raffinose to prevent colloidal-osmotic swelling of the erythrocytes that could be induced by HA-mediated leakage) (Melikyan et al., 1999). The medium was replaced with DMEM supplemented with 7.5% FBS. After incubation for 15 min at 37 °C, hemadsorption and the transfer of fluorescence were observed with a phase-contrast microscope and a fluorescence microscope, respectively.

Acknowledgments

Support for our work has been provided by NIH Public Service Grant AI66870 (D.A.S.), NIH/NIAID contract HHSN266200700006C, and the Scottish Funding Council (R.J.R.).

References

Appleyard, G., Maber, H.B., 1974. Plaque formation by influenza viruses in the presence of trypsin. J. Gen. Virol. 25 (3), 351–357.
Armstrong, R.T., Kushnir, A.S., White, J.M., 2000. The transmembrane domain of influenza hemagglutinin exhibits a stringent length requirement to support the hemifusion to fusion transition. J. Cell Biol. 151 (2), 425–437.
Bizebard, T., Gigant, B., Rigolet, P., Rasmussen, B., Diat, O., Bosecke, P., Wharton, S.A., Skehel, J.J., Knossow, M., 1995. Structure of influenza virus haemagglutinin complexed with a neutralizing antibody. Nature 376 (6535), 92–94.
Blasco, R., Moss, B., 1995. Selection of recombinant vaccinia viruses on the basis of plaque formation. Gene 158 (2), 157–162.
Bullough, P.A., Hughson, F.M., Skehel, J.J., Wiley, D.C., 1994. Structure of influenza haemagglutinin at the pH of membrane fusion. Nature 371 (6492), 37–43.
Burger, K.N., Wharton, S.A., Demel, R.A., Verkleij, A.J., 1991. The interaction of synthetic analogs of the N-terminal fusion sequence of influenza virus with a lipid monolayer. Comparison of fusion-active and fusion-defective analogs. Biochim. Biophys. Acta 1065 (2), 121–129.
Chang, D.K., Cheng, S.F., Deo Trivedi, V., Yang, S.H., 2000. The amino-terminal region of the fusion peptide of influenza virus hemagglutinin HA2 inserts into sodium dodecyl sulfate micelle with residues 16-18 at the aqueous boundary at acidic pH. Oligomerization and the conformational flexibility. J. Biol. Chem. 275 (25), 19150–19158.
Chang, D.K., Cheng, S.F., Kantchev, E.A., Lin, C.H., Liu, Y.T., 2008. Membrane interaction and structure of the transmembrane domain of influenza hemagglutinin and its fusion peptide complex. BMC Biol. 6, 2.
Chen, J., Lee, K.H., Steinhauer, D.A., Stevens, D.J., Skehel, J.J., Wiley, D.C., 1998. Structure of the hemagglutinin precursor cleavage site, a determinant of influenza pathogenicity and the origin of the labile conformation. Cell 95 (3), 409–417.
Chen, J., Skehel, J.J., Wiley, D.C., 1999. N- and C-terminal residues combine in the fusion-pH influenza hemagglutinin HA(2) subunit to form an N cap that terminates the triple-stranded coiled coil. Proc. Natl. Acad. Sci. U.S.A. 96 (16), 8967–8972.
Cheng, S.F., Kantchev, A.B., Chang, D.K., 2003. Fluorescence evidence for a loose self-assembly of the fusion peptide of influenza virus HA2 in the lipid bilayer. Mol. Membr. Biol. 20 (4), 345–351.
Cross, K.J., Wharton, S.A., Skehel, J.J., Wiley, D.C., Steinhauer, D.A., 2001. Studies on influenza haemagglutinin fusion peptide mutants generated by reverse genetics. Embo J. 20 (16), 4432–4442.
Daniels, R.S., Douglas, A.R., Skehel, J.J., Wiley, D.C., 1983. Analyses of the antigenicity of influenza haemagglutinin at the pH optimum for virus-mediated membrane fusion. J. Gen. Virol. 64 (Pt 8), 1657–1662.
Daniels, R.S., Downie, J.C., Hay, A.J., Knossow, M., Skehel, J.J., Wang, M.L., Wiley, D.C., 1985. Fusion mutants of the influenza virus hemagglutinin glycoprotein. Cell 40 (2), 431–439.
Durrer, P., Galli, C., Hoenke, S., Corti, C., Gluck, R., Vorherr, T., Brunner, J., 1996. H+-induced membrane insertion of influenza virus hemagglutinin involves the HA2 amino-terminal fusion peptide but not the coiled coil region. J. Biol. Chem. 271 (23), 13417–13421.
Ellens, H., Bentz, J., Mason, D., Zhang, F., White, J.M., 1990. Fusion of influenza hemagglutinin-expressing fibroblasts with glycophorin-bearing liposomes: role of hemagglutinin surface density. Biochemistry 29 (41), 9697–9707.
Gething, M.J., Doms, R.W., York, D., White, J., 1986. Studies on the mechanism of membrane fusion: site-specific mutagenesis of the hemagglutinin of influenza virus. J. Cell Biol. 102 (1), 11–23.
Gray, C., Tatulian, S.A., Wharton, S.A., Tamm, L.K., 1996. Effect of the N-terminal glycine on the secondary structure, orientation, and interaction of the influenza hemagglutinin fusion peptide with lipid bilayers. Biophys. J. 70 (5), 2275–2286.
Han, X., Tamm, L.K., 2000. A host-guest system to study structure-function relationships of membrane fusion peptides. Proc. Natl. Acad. Sci. U.S.A. 97 (24), 13097–13102.
Han, X., Steinhauer, D.A., Wharton, S.A., Tamm, L.K., 1999. Interaction of mutant influenza virus hemagglutinin fusion peptides with lipid bilayers: probing the role of hydrophobic residue size in the central region of the fusion peptide. Biochemistry 38 (45), 15052–15059.
Han, X., Bushweller, J.H., Cafiso, D.S., Tamm, L.K., 2001. Membrane structure and fusion-triggering conformational change of the fusion domain from influenza hemagglutinin. Nat. Struct. Biol. 8 (8), 715–720.
Harrison, S.C., 2008. Viral membrane fusion. Nat. Struct. Mol. Biol. 15 (7), 690–698.
Harter, C., James, P., Bachi, T., Semenza, G., Brunner, J., 1989. Hydrophobic binding of the ectodomain of influenza hemagglutinin to membranes occurs through the "fusion peptide". J. Biol. Chem. 264 (11), 6459–6464.
Hsu, C.H., Wu, S.H., Chang, D.K., Chen, C., 2002. Structural characterizations of fusion peptide analogs of influenza virus hemagglutinin. Implication of the necessity of a helix-hinge-helix motif in fusion activity. J. Biol. Chem. 277 (25), 22725–22733.
Kemble, G.W., Danieli, T., White, J.M., 1994. Lipid-anchored influenza hemagglutinin promotes hemifusion, not complete fusion. Cell 76 (2), 383–391.

Kielian, M., Rey, F.A., 2006. Virus membrane-fusion proteins: more than one way to make a hairpin. Nat. Rev. Microbiol. 4 (1), 67–76.
Klenk, H.D., Rott, R., Orlich, M., Blodorn, J., 1975. Activation of influenza A viruses by trypsin treatment. Virology 68 (2), 426–439.
Korte, T., Epand, R.F., Epand, R.M., Blumenthal, R., 2001. Role of the Glu residues of the influenza hemagglutinin fusion peptide in the pH dependence of fusion activity. Virology 289 (2), 353–361.
Lai, A.L., Tamm, L.K., 2007. Locking the kink in the influenza hemagglutinin fusion domain structure. J. Biol. Chem. 282 (33), 23946–23956.
Lai, A.L., Park, H., White, J.M., Tamm, L.K., 2006. Fusion peptide of influenza hemagglutinin requires a fixed angle boomerang structure for activity. J. Biol. Chem. 281 (9), 5760–5770.
Lamb, R.A., Jardetzky, T.S., 2007. Structural basis of viral invasion: lessons from paramyxovirus F. Curr. Opin. Struct. Biol. 17 (4), 427–436.
Lau, W.L., Ege, D.S., Lear, J.D., Hammer, D.A., DeGrado, W.F., 2004. Oligomerization of fusogenic peptides promotes membrane fusion by enhancing membrane destabilization. Biophys. J. 86 (1 Pt. 1), 272–284.
Lazarowitz, S.G., Choppin, P.W., 1975. Enhancement of the infectivity of influenza A and B viruses by proteolytic cleavage of the hemagglutinin polypeptide. Virology 68 (2), 440–454.
Lear, J.D., DeGrado, W.F., 1987. Membrane binding and conformational properties of peptides representing the NH2 terminus of influenza HA-2. J. Biol. Chem. 262 (14), 6500–6505.
Li, Y., Han, X., Tamm, L.K., 2003. Thermodynamics of fusion peptide-membrane interactions. Biochemistry 42 (23), 7245–7251.
Li, Y., Han, X., Lai, A.L., Bushweller, J.H., Cafiso, D.S., Tamm, L.K., 2005. Membrane structures of the hemifusion-inducing fusion peptide mutant G1S and the fusion-blocking mutant G1V of influenza virus hemagglutinin suggest a mechanism for pore opening in membrane fusion. J. Virol. 79 (18), 12065–12076.
Li, Z.N., Lee, B.J., Langley, W.A., Bradley, K.C., Russell, R.J., Steinhauer, D.A., 2008. Length requirements for membrane fusion of influenza virus hemagglutinin peptide linkers to transmembrane or fusion peptide domains. J. Virol. 82 (13), 6337–6348.
Lin, Y.P., Wharton, S.A., Martin, J., Skehel, J.J., Wiley, D.C., Steinhauer, D.A., 1997. Adaptation of egg-grown and transfectant influenza viruses for growth in mammalian cells: selection of hemagglutinin mutants with elevated pH of membrane fusion. Virology 233 (2), 402–410.
Macosko, J.C., Kim, C.H., Shin, Y.K., 1997. The membrane topology of the fusion peptide region of influenza hemagglutinin determined by spin-labeling EPR. J. Mol. Biol. 267 (5), 1139–1148.
Melikyan, G.B., Brener, S.A., Ok, D.C., Cohen, F.S., 1997. Inner but not outer membrane leaflets control the transition from glycosylphosphatidylinositol-anchored influenza hemagglutinin-induced hemifusion to full fusion. J. Cell Biol. 136 (5), 995–1005.
Melikyan, G.B., Lin, S., Roth, M.G., Cohen, F.S., 1999. Amino acid sequence requirements of the transmembrane and cytoplasmic domains of influenza virus hemagglutinin for viable membrane fusion. Mol. Biol. Cell 10 (6), 1821–1836.
Melikyan, G.B., Markosyan, R.M., Roth, M.G., Cohen, F.S., 2000. A point mutation in the transmembrane domain of the hemagglutinin of influenza virus stabilizes a hemifusion intermediate that can transit to fusion. Mol. Biol. Cell 11 (11), 3765–3775.
Morris, S.J., Sarkar, D.P., White, J.M., Blumenthal, R., 1989. Kinetics of pH-dependent fusion between 3T3 fibroblasts expressing influenza hemagglutinin and red blood cells. Measurement by dequenching of fluorescence. J. Biol. Chem. 264 (7), 3972–3978.
Murata, M., Sugahara, Y., Takahashi, S., Ohnishi, S., 1987. pH-dependent membrane fusion activity of a synthetic twenty amino acid peptide with the same sequence as that of the hydrophobic segment of influenza virus hemagglutinin. J. Biochem. 102 (4), 957–962.
Nobusawa, E., Hishida, R., Murata, M., Kawasaki, K., Ohnishi, S., Nakajima, K., 1995. The role of acidic residues in the "fusion segment" of influenza A virus hemagglutinin in low-pH-dependent membrane fusion. Arch. Virol. 140 (5), 865–875.
Orlich, M., Rott, R., 1994. Thermolysin activation mutants with changes in the fusogenic region of an influenza virus hemagglutinin. J. Virol. 68 (11), 7537–7539.
Qiao, H., Armstrong, R.T., Melikyan, G.B., Cohen, F.S., White, J.M., 1999. A specific point mutant at position 1 of the influenza hemagglutinin fusion peptide displays a hemifusion phenotype. Mol. Biol. Cell 10 (8), 2759–2769.
Rafalski, M., Ortiz, A., Rockwell, A., van Ginkel, L.C., Lear, J.D., DeGrado, W.F., Wilschut, J., 1991. Membrane fusion activity of the influenza virus hemagglutinin: interaction of HA2 N-terminal peptides with phospholipid vesicles. Biochemistry 30 (42), 10211–10220.
Skehel, J.J., Bayley, P.M., Brown, E.B., Martin, S.R., Waterfield, M.D., White, J.M., Wilson, I.A., Wiley, D.C., 1982. Changes in the conformation of influenza virus hemagglutinin at the pH optimum of virus-mediated membrane fusion. Proc. Natl. Acad. Sci. U.S.A. 79 (4), 968–972.
Skehel, J.J., Cross, K., Steinhauer, D., Wiley, D.C., 2001. Influenza fusion peptides. Biochem. Soc. Trans. 29 (Pt. 4), 623–626.
Steinhauer, D.A., Wharton, S.A., Wiley, D.C., Skehel, J.J., 1991. Deacylation of the hemagglutinin of influenza A/Aichi/2/68 has no effect on membrane fusion properties. Virology 184 (1), 445–448.
Steinhauer, D.A., Wharton, S.A., Skehel, J.J., Wiley, D.C., 1995. Studies of the membrane fusion activities of fusion peptide mutants of influenza virus hemagglutinin. J. Virol. 69 (11), 6643–6651.
Thoennes, S., Li, Z.N., Lee, B.J., Langley, W.A., Skehel, J.J., Russell, R.J., Steinhauer, D.A., 2008. Analysis of residues near the fusion peptide in the influenza hemagglutinin structure for roles in triggering membrane fusion. Virology 370 (2), 403–414.
Ujike, M., Nakajima, K., Nobusawa, E., 2005. Influence of additional acylation site(s) of influenza B virus hemagglutinin on syncytium formation. Microbiol. Immunol. 49 (4), 355–359.
Vareckova, E., Cox, N., Klimov, A., 2002. Evaluation of the subtype specificity of monoclonal antibodies raised against H1 and H3 subtypes of human influenza A virus hemagglutinins. J. Clin. Microbiol. 40 (6), 2220–2223.
Weissenhorn, W., Hinz, A., Gaudin, Y., 2007. Virus membrane fusion. FEBS Lett. 581 (11), 2150–2155.
Wharton, S.A., Martin, S.R., Ruigrok, R.W., Skehel, J.J., Wiley, D.C., 1988. Membrane fusion by peptide analogues of influenza virus haemagglutinin. J. Gen. Virol. 69 (Pt. 8), 1847–1857.
Wharton, S.A., Calder, L.J., Ruigrok, R.W., Skehel, J.J., Steinhauer, D.A., Wiley, D.C., 1995. Electron microscopy of antibody complexes of influenza virus haemagglutinin in the fusion pH conformation. Embo J. 14 (2), 240–246.
White, J.M., Delos, S.E., Brecher, M., Schornberg, K., 2008. Structures and mechanisms of viral membrane fusion proteins: multiple variations on a common theme. Crit. Rev. Biochem. Mol. Biol. 43 (3), 189–219.
Wiley, D.C., Skehel, J.J., 1987. The structure and function of the hemagglutinin membrane glycoprotein of influenza virus. Annu. Rev. Biochem. 56, 365–394.
Wilson, I.A., Skehel, J.J., Wiley, D.C., 1981. Structure of the haemagglutinin membrane glycoprotein of influenza virus at 3 A resolution. Nature 289 (5796), 366–373.
Yewdell, J.W., Taylor, A., Yellen, A., Caton, A., Gerhard, W., Bachi, T., 1993. Mutations in or near the fusion peptide of the influenza virus hemagglutinin affect an antigenic site in the globular region. J. Virol. 67 (2), 933–942.